1st Virtual European Conference on Fracture

True Stress-strain Curves for HSLA Steel Weldment – Iteration Procedure Based on DIC and FEM

B. Younise[a], A. Sedmak[b]*, N. Milosević[b], M. Rakin[c], B. Medjo[c]

[a] Faculty of Engineering, Elmergib University, Alkhoms, Libya
[b] Faculty of Mechanical Engineering, University of Belgrade, Serbia
[c] Faculty of technology and Metallurgy, University of Belgrade, Serbia

Abstract

True stress-strain curves of HSLA steel welded joint regions were estimated by using numerical simulation of strains measured by DIC and special iteration procedure to match the results. Strains were measured at certain level of loading in all regions of welded joint with different tensile properties, namely base metal (BM), weld metal (WM) and two subzones of Heat-Affected-Zone (fine grain, FGHAZ, and coarse grain – CGHAZ). By converting engineering stress (load divided by initial cross section area) into true stress, experimental true stress-true strain curves are obtained and used as initial iteration for the Finite Element Method (FEM) simulation, after being fitted by the power law relation for stress-strain curves. Obtained results are then compared with the experimental results to find the differences and make appropriate correction in power law curves and make as many iterations as needed before the differences become small enough. This procedure has been verified by an example of welded tensile panel.

1. Introduction

Micromechanical modelling of local damage, i.e. crack initiation and propagation in ductile materials, usually requires a combination of experimental and numerical work, as already elaborated by authors [1-7]. Crack initiation

---

* Corresponding author
  E-mail address: aleksandarsedmak@gmail.com

and propagation can be numerically simulated by applying micromechanical models such as a complete Gurson model (CGM), directly implemented in numerical FE codes or through user subroutines to simulate local damage, [8].

If crack is located in welded joint it is of utmost importance to know tensile properties of all its regions (BM, WM, HAZ), as precisely as possible. When ductile fracture is considered, engineering curves are not appropriate, since the simulation of large plastic strains requires true stress-true strain curves.

In doctoral thesis of the first author, [9], the crack initiation and propagation has been analyzed in details in welded single edge notched bend 3PB specimens and TPs with a pre-crack in WM or HAZ. The aim was to determine the effects of mechanical heterogeneity and constraints on ductile crack initiation and propagation in high strength steel weldments using the same and different specimen geometries and loading configurations, [9]. In addition, the scope of numerical analysis of local damage in weldments was also to analyze the transferability of material damage parameters among different welded specimens. The 2D and 3D FE analyses were carried out for various welded specimens using ABAQUS. The effect of heterogeneity was numerically analyzed by considering welded specimens with pre-cracks in WM and HAZ. Moreover, constraint effect on fracture behavior was analyzed as well, [9]. Anyhow, the common problem in all these investigations was how to evaluate tensile properties in different zones of welded joint, i.e. in BM, WM, CG and FG HAZ, which is the focus of this paper. Thereby, one should keep in mind that this is not a simple task due to metallurgical and strength heterogeneity, especially for narrow heat affected subzones, when it is practically impossible to accomplish it experimentally, beacuse even with micro-specimens one could gets valid results only for longitudinal weldment direction.

2. Experimental analysis of welded joint

The base metal in this research was a high-strength low-alloyed steel, produced in Slovenia, brand name Niomol 490K, used mostly for pressure vessels, with composition given in Table 1, together with the consumable VAC 60 Ni.

Table 1 Chemical composition of base metal, NIOMOL 490K and consumable in weight %.

Material	C	Si	Mn	P	S	Mo	Cr	Ni
NIOMOL 490K	0.123	0.33	0.56	0.003	0.002	0.34	0.57	0.13
VAC 60 Ni	0.096	0.58	1.24	0.013	0.016	0.02	0.07	0.03

Shielded metal arc welding process (SMAW) was used with consumable VAC 60Ni, wire diameter was 1.2 mm. A mixture of shielding gases was used to have acicular ferrite for obtaining higher toughness. Fatigue pre-crack is positioned in WM or HAZ and K welded joint shape to make easier positioning of a crack in HAZ.

Smooth tensile plate was cut transversally from welded plate and tested at room temperature (Figure 1). The specimen was pulled longitudinally, while force and remote displacement were monitored by testing machine. At the same time, longitudinal strains at different loads were measured using ARAMIS stereometric measuring system (www.gom.com), applied recenlty to solve different problems, [10-12]. Engineering remote stress - true strain data for welded joint regions (BM, WM and HAZ) was obtained from ARAMIS measured strains with corresponding applied force. Strains in each region at corresponding forces were calculated by averaging strains along measured line. Then, engineering remote stress was calculated at corresponding strain using initial cross section of tested specimen, as described in more details [9]. The engineering remote stress (σ) was then converted into the true stress (σ_T) using the expression: $\sigma_T = \sigma(1+\varepsilon)$, where ε is the true strain.
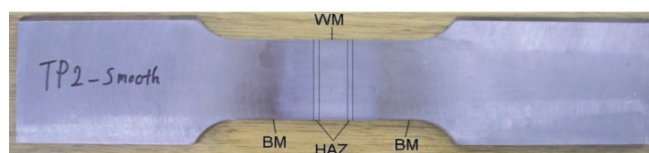

Figure 1 Welded **Tensile** Panel, as prepared for testing

3. Numerical simulation of welded joint tensile properties

Engineering stress-strain curves are sometimes represented by bilinear relationship, estimated by using iteration procedure to match experimental and numerical results, as presented in [10, 13-14]. However, this type of relation can't provide accurate approximation for ductile material behaviour beyond ultimate stress, which are required for micromechanical modeling (CGM). In addition, mechanical properties of welded joint regions may be difficult to be determined in the direction of applied force, especially when the welded joint is subjected to transversally applied load. Therefore, new, combined experimental and numerical procedure is presented here as alternative method to estimate mechanical properties for various welded joint regions using the power law relation for stress-strain curves. Starting point were the results of DIC measurement, shown for different load levels in Fig. 2, as distribution along the transverse direction. Measured and calculated strains, Fig. 2, were then used as the reference for numerical simulation. Toward this aim, the smooth tensile specimen was numerically modeled using ABAQUS with three-dimensional eight-node brick elements to estimate strains in various regions. Finer mesh has been used for the regions where the strains were measured. Due to the symmetry, only one quarter of specimen was numerically modeled as shown in Fig. 3 with boundary conditions and specimen geometry. One side of specimen was fixed, while prescribed displacement was applied to the other one representing applied load.
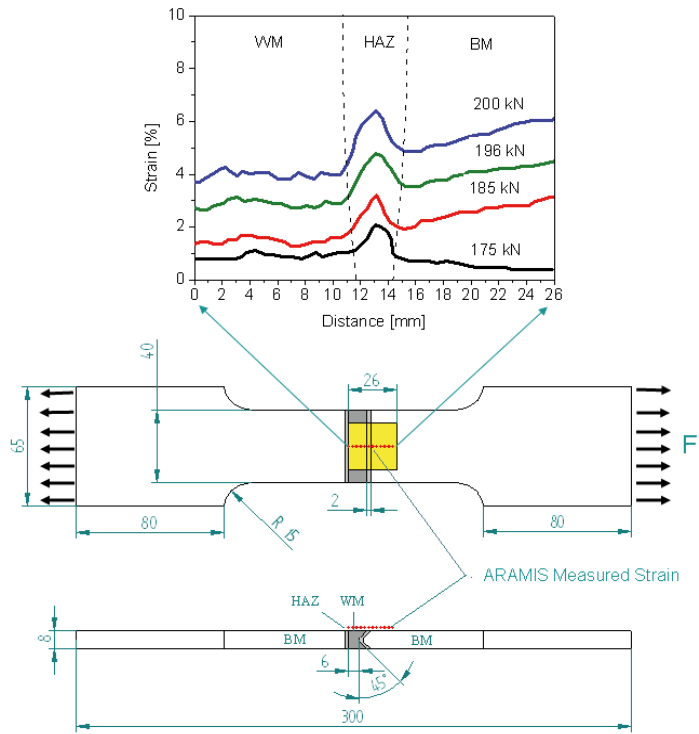

Figure 2 Geometry of smooth tensile specimen with experimental ARAMIS measured strain

True stress-strain behavior of materials was found to follow Hollomon power law up to maximum load according to expressions:

$$\varepsilon = \varepsilon_e + \varepsilon_p$$
$$\sigma = E\varepsilon_e \ if \ \sigma \le \sigma_{YS}$$
$$\sigma = K\varepsilon^n \ if \ \sigma > \sigma_{YS}$$

where ε_e and ε_p are elastic and plastic strains, respectively, E is Young's modulus, σ_{YS} is the yield strength, K is strength coefficient and n is material hardening exponent.
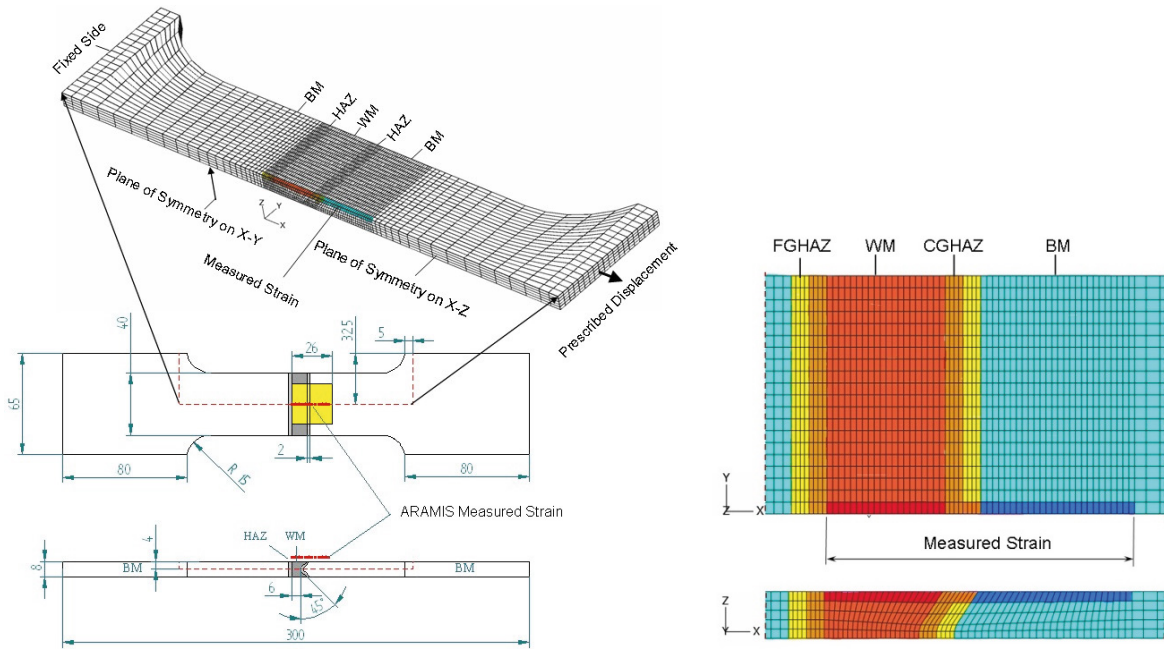
Figure 3 (a) Finite element mesh of quarter tensile specimen and (b) detailed mesh

The proper combination of tensile properties (E, σ_{YS}) and Hollomon parameters (K and n) were determined by varying them up to obtaining good agreement between numerical and experimental results at different loads. About 25 iterations were performed to obtain the proper combination of elastic and plastic properties. The initial iteration values of E, σ_{YS}, K and n were estimated from the obtained experimental true stress - strain curves in Figure 7a. The mechanical properties (E and σ_{YS}) and Hollomon parameters (K and n) are given in Table 2 for three iterations as example for performing iteration procedure. Experimental fracture stress and strain were used to estimate large strains beyond ultimate stress. Then, the whole data of true stress-strain curves have been fitted by Harris model, which has given the closest fitting curves to data. The Harris model is given as $y=1/(a+b \cdot x^c)$, where a, b and c are parameters, which are given in Table 3 for BM, CGHAZ, FGHAZ and WM and for three iterations in order to compare the results among iterations. The iteration 3 in Tables 2 and 3 provides good matching between numerical and experimental results.

Table 2 Mechanical properties of the materials for 3 numerical iterations.

Material	Iteration	E (MPa)	σ_{YS} (MPa)	n	K (MPa)
	1	169320	459	0.1	944
WM	2	195000	550	0.08	971
	3	200000	530	0.21	1255
	1	190037	459	0.11	935
CGHAZ	2	200000	530	0.09	947
	3	203000	550	0.17	968
	1	190037	459	0.11	935
FGHAZ	2	200000	500	0.08	901
	3	195000	500	0.23	1217
	1	176972	459	0.11	929
BM	2	202000	540	0.1	940
	3	202900	520	0.22	1157

Table 3 Harris model constants for true stress- true strain curves for 3 iterations

Material	Iteration	a	b	c
	1	0.07022	-0.06923	0.00242
BM	2	0.01353	-0.01246	0.00943
	3	0.02719	-0.00189	0.16269
	1	0.05325	-0.05228	0.00329
CGHAZ	2	0.01246	-0.0114	0.00952
	3	0.00217	-0.00119	0.25879
	1	0.05325	-0.05228	0.00329
FGHAZ	2	0.01369	-0.01258	0.00799
	3	0.00551	-0.00472	0.05847
	1	0.05175	-0.05079	0.00328
WM	2	0.01289	-0.01186	0.00756
	3	0.00438	-0.0036	0.06696

Figure 4 shows true stress - true strain curves in the first and the last iteration for all regions. Figures 5 and 6 show strain distribution at various loads (175 and 200 kN, respectively), in the same way, whereas comparison between tested specimen and numerical longitudinal strain distribution for 3 iterations at the same overall elongation ($\Delta L = 16$ mm) is shown elsewhere, [8], indicating good agreement between numerical and experimental results, with necking at about the same position.
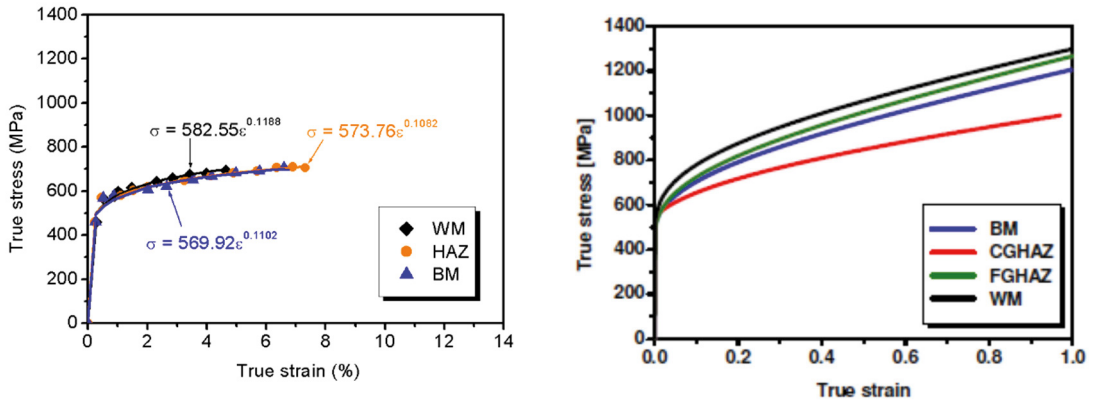

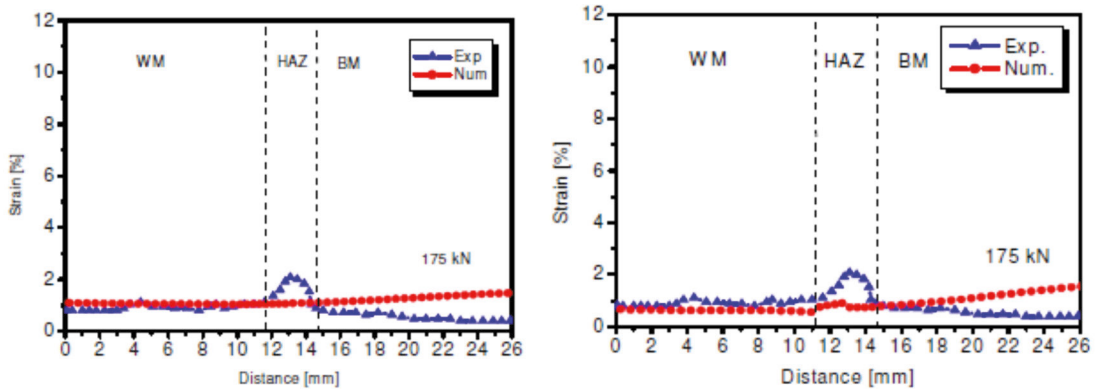Figure 4. The 1st and 3rd iteration for true stress – true strain curves for all regions of welded joint

Figure 5. The 1st and 3rd iteration for strain distribution – load 175 KN
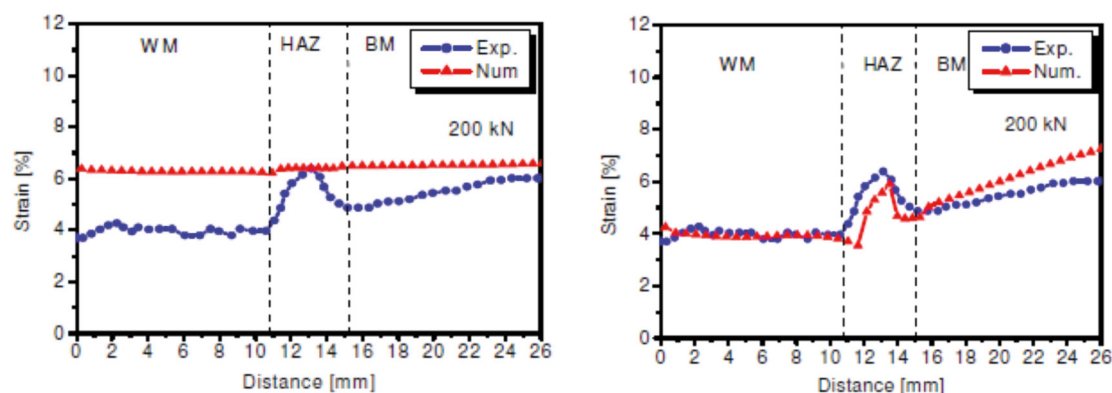
Fig. 6. The 1st and 3rd iteration for strain distribution – load 200 KN

4. Conclusions

Based on the results presented here for the true stress-strain curves estimated by using DIC and FEM, one can conclude the following:

- Iterative procedure of matching experimental and numerical results has proven to be efficient method of estimating true stress – true strain curves for different regions of welded joints
- 3 iterations were enough making this procedure simple, but one needs more experience to make this conclusion general one.
- Procedure is relatively simple and efficient, especially for cases when other means of true stress-strain curve estimation are limited or not existing.

5. Literature

1. A. Sedmak, Computational fracture mechanics: An overview from early efforts to recent achievements, Fatigue Fract Eng Mater Struct. 2018; 41: 2438–2474.
2. B. Younise, M. Rakin, N. Gubeljak, B. Medjo, A. Sedmak, Effect of material heterogeneity and constraint conditions on ductile fracture resistance of welded joint zones - Micromechanical assessment, Engineering failure analysis 2017, 82 ():435-445
3. B. Younise, M. Rakin, B. Međo, N. Gubeljak, D. Kozak, A. Sedmak, Numerical analysis of constraint effect on ductile tearing in strength mismatched welded CCT specimens using micromechanical approach, Technical gazette, Vol 18 (3), 2011: 333-340
4. B. Younise, A. Sedmak, M. Rakin, N. Gubeljak, B. Medjo, M. Burzić, M. Zrilić, Micromechanical analysis of mechanical heterogeneity effect on the ductile tearing of weldments, Materials and design, 2012, 37 ():193-201
5. Younise Bashir, Rakin Marko, Gubeljak Nenad, Medjo Bojan, Sedmak Aleksandar, Numerical prediction of ductile fracture resistance of welded joint zones, 21st European Conference on Fracture, Procedia Structural Integrity, 2016, 2 ():753-760
6. B. Younise, M. Rakin, N. Gubeljak, B. Medjo, A. Sedmak, Numerical Simulation of Constraint Effect on Fracture Initiation in Welded Specimens Using a Local Damage Model, Structural Integrity and Life, Vol. 11 (1) 2011: 51-56
7. B.S. Younise, A. Sedmak, Micromechanical Study of Ductile Fracture Initiation and Propagation on Welded Tensile Specimen with a Surface Pre-Crack in Weld Metal, Structural Integrity and Life, Vol. 14 (3) 2014: 185-191
8. Zhang, Z.L., Thaulow, C., Ødegard. J., A complete Gurson model approach for ductile fracture. Eng. Fract. Mech. 67, 2000, pp. 155-168.
9. B. Younise, Micromechanical fracture analysis of high strength steel weldments doctoral thesis, University of Belgrade, 2014
10. M. Milosevic, N. Mitrovic, R. Jovicic, A. Sedmak, T. Maneski, A. Petrovic, T. Aburaga, Measurement of Local Tensile Properties of Welded Joint Using Digital Image Correlation Method, Chemicke listy 2012, 106 ():S485-S488
11. Glaser, Bruno; Predan, Jozef; Kozak, Drazan; et al. Comparison between Stereo Optical Strain Measurements and Finite Element Results in Stress Concentration Zones, TECHNICAL GAZETTE 2019, Volume: 26, (5):1346-1352
12. Nenad Mitrovic, Milos Milosevic, Aleksandar Sedmak, Aleksandar Petrovic, Radica Prokic-Cvetkovic Application and Mode of Operation of Non-Contact Stereometric Measuring System of Biomaterials, FME Transactions (2011) 39, 55-60
13. R. Jovicic, S.A. Sedmak, I. Samardzic, A. Sedmak, U. Tatic, M. Milosevic, Possibilities of Predicting the Behaviour of Ferrite-Austenite Welded Joints in Pressure Equipment During Exploitation, Technical Gazette 2017 24 (5):1361-1368
14. Nenad Milošević, Miloš Milošević, Simon Sedmak, Uroš Tatić, Nenad Mitrović, Sergej Hloch, Radomir Jovičić, Digital image correlation in analysis of deformation ability of welded joints, Tehnički vjesnik 21, 2 (2014), 447-450